

Conditional mutation of the ErbB2 (HER2) receptor in cardiomyocytes leads to dilated cardiomyopathy

Cemil Özcelik*[†], Bettina Erdmann*, Bernhard Pilz[†], Nina Wettschreck[‡], Stefan Britsch*, Norbert Hübner*, Kenneth R. Chien[§], Carmen Birchmeier*[¶], and Alistair N. Garratt*

*Max Delbrück Center for Molecular Medicine, Robert-Rössle-Strasse 10, 13125 Berlin, Germany; [†]Franz-Volhard-Klinik, Wiltbergstrasse 50, 13125 Berlin, Germany; [‡]University of Heidelberg, Institute of Pharmacology, 69120 Heidelberg, Im Neuenheimer Feld 366, Germany; and [§]Department of Medicine, University of California at San Diego, 9500 Gilman Drive, La Jolla, CA 92093-0613

Communicated by Michael H. Wigler, Cold Spring Harbor Laboratory, Cold Spring Harbor, NY, April 26, 2002 (received for review February 21, 2002)

The *ErbB2* (*Her2*) proto-oncogene encodes a receptor tyrosine kinase, which is frequently amplified and overexpressed in human tumors. ErbB2 provides the target for a novel and effective antibody-based therapy (Trastuzumab/Herceptin) used for the treatment of mammary carcinomas. However, cardiomyopathies develop in a proportion of patients treated with Trastuzumab, and the incidence of such complications is increased by combination with standard chemotherapy. Gene ablation studies have previously demonstrated that the ErbB2 receptor, together with its coreceptor ErbB4 and the ligand Neuregulin-1, are essential for normal development of the heart ventricle. We use here Cre-loxP technology to mutate *ErbB2* specifically in ventricular cardiomyocytes. Conditional mutant mice develop a severe dilated cardiomyopathy, with signs of cardiac dysfunction generally appearing by the second postnatal month. We infer that signaling from the ErbB2 receptor, which is enriched in T-tubules in cardiomyocytes, is crucial for adult heart function. Conditional *ErbB2* mutant mice provide a model of dilated cardiomyopathy. In particular, they will allow a rigorous assessment of the role of ErbB2 in the heart and provide insight into the molecular mechanisms that underlie the adverse effects of anti-ErbB2 antibodies.

Dilated cardiomyopathies are an important cause of heart failure (1). Affected patients present with ventricular dilatation, thinned ventricle walls, and reductions in pumping efficiency, leading typically to congestive heart failure and premature death. Diverse mechanisms can cause dilated cardiomyopathies leading to heart failure, like ischemic injury or infection. Epidemiological studies suggest that 25–30% of dilated cardiomyopathies are inherited (1). Among the genes that, when mutated, cause dilated cardiomyopathies in humans and mice are those encoding intrasarcomeric and extrasarcomeric cytoskeletal proteins (1, 2). Mutations in these known genes account for only a minor proportion of the heritable cardiomyopathies in humans. In the mouse, mutations in the bradykinin-B₂ and serotonin-2B receptor genes also cause dilated cardiomyopathies (3, 4), whereas components of calcium homeostasis or the β -adrenergic system can, when altered genetically, prevent their development (5). Thus, alterations in the fine tuning of contractility or the adaptive responses to cardiac load can contribute to the development of this disease.

The ErbB2 receptor tyrosine kinase was originally identified due to its potent oncogenic activity (6, 7). Biochemical studies and gene ablation in the mouse revealed that ErbB2 functions as a coreceptor in Neuregulin signaling (6, 8, 9). ErbB2 heteromerizes with ErbB3 and ErbB4, the high-affinity receptors for Neuregulin, and is essential for transmission of the Neuregulin signal (6). Moreover, ErbB2 participates in signaling of the epidermal growth factor receptor, gp130/cytokine receptors and G-coupled receptors in cultured cells (10). ErbB2/4 receptors and Neuregulin-1 are essential for heart development: mutations in *Neuregulin-1*, *ErbB2*, or *ErbB4* in mice result in impaired ventricular trabeculation, causing midgestation lethality. During development, Neuregulin-1 signals are provided by the endo-

cardium and received by the ErbB2/ErbB4 receptors in the myocardium (8, 11). In addition, the ErbB2/ErbB4 receptors as well as Neuregulins remain expressed in the adult heart.

Overexpression or amplification of *ErbB2* is frequently associated with carcinomas, prompting its selection as a target for novel therapeutic agents (6, 7). The humanized antibody, Trastuzumab (also known as Herceptin), is directed against the extracellular domain of human ErbB2. Trastuzumab recognizes ErbB2 on the cell surface, dimerizes the receptor, and rapidly promotes its internalization and down-regulation (12). Trastuzumab elicits an antiproliferative effect in cells overexpressing human ErbB2 (12). *In vivo*, recruitment of the immune system might enhance its antitumorigenic properties (12). Combination treatment of Trastuzumab and chemotherapeutics is an effective clinical therapy for malignant breast tumors that overexpress ErbB2. It lengthens time to disease progression, life expectancy, and reduces the risk of death (13). A fraction of patients that undergo such a combination treatment, however, develops cardiac dysfunction (13). This observation might indicate that the target, ErbB2, functions in homeostasis of the adult heart. The effects of Trastuzumab on heart function cannot be analyzed in animal models as the antibody recognizes specifically the human ErbB2 protein only.

To address the function of ErbB2 in the postnatal heart, we mutated *ErbB2* specifically in cardiomyocytes of mice. For this purpose, mice that express Cre recombinase under the control of the *MLC2v* (*myosin light chain 2v*) locus were used (14, 15). Conditional *ErbB2* mutants were born at the expected Mendelian frequency, and most reached adulthood but developed severe dilated cardiomyopathy with a typical onset in the second month of age. Our analysis indicates ErbB2 is not required for survival of cardiomyocytes and demonstrates a function of ErbB2 in normal heart physiology. Impairing ErbB2 activity in the heart can thus directly cause cardiomyopathy and heart failure.

Materials and Methods

Mouse Strains. The *ErbB2*^{fllox}, *ErbB2*⁻, and *MLC2v*^{cre} alleles have been described (14, 16, 17). Genotyping of the animals was performed by PCR and occasionally verified by Southern blot analysis. Conditional mutant mice with the genotype *MLC2v*^{cre/+}; *ErbB2*^{fllox/-} displayed reduced survival. Sixteen percent died within the first two postnatal weeks (9 of a total of 58); the remainder reached adulthood. A cohort of 22 conditional mutant animals was set aside to assess the frequency of sudden death, and of those, 27% died before reaching the age of 6 mo. Moreover, a proportion of conditional mutant mice (20%) died during echocardiographic or ECG examinations (3 of 15). Three genotypes were used as control animals: *MLC2v*^{cre/+}; *ErbB2*^{fllox/+} (Southern hybridization, echocardiography), *ErbB2*^{fllox/-} (echocardiography and microarray analysis), and *ErbB2*^{fllox/+} (echocardiography).

[¶]To whom reprint requests should be addressed. E-mail: cbirch@mdc-berlin.de.

Immunostaining and Histology. Tissues were isolated from mice perfused with 4% paraformaldehyde, cryoprotected with 20% sucrose, and frozen in Oct compound (Sakura, Torrance, CA). Cryosections (12 μm) were stained with the following antibodies: rabbit polyclonal against ErbB2 (Santa Cruz Biotechnology; 1:100), ErbB4 (Santa Cruz Biotechnology; 1:100), anti-ErbB4 serum no. 0616 (a gift from Cary Lai, Scripps Research Institute, San Diego, CA; 1:1,500), mouse monoclonal anti-vinculin (Sigma; 1:300), and Cy2- or Cy3- conjugated secondary antibodies (Dianova, Hamburg, Germany; 1:200). T-tubule staining using anti-ErbB4 antibodies was observed with two additional rabbit polyclonal sera raised against ErbB4 (sera nos. 0615 and 0618; gifts from Cary Lai), i.e., all anti-ErbB4 sera tested. T-tubule staining with anti-ErbB2 was reproducibly observed with one antibody batch (Santa Cruz Biotechnology, lot no. A087), whereas results obtained with a second batch were variable (Santa Cruz Biotechnology, lot no. H145). Histological, BrdUrd, and terminal deoxynucleotidyltransferase-mediated dUTP end labeling (TUNEL) and electron microscopical analyses were performed as described (16).

Determination of Cre-Mediated Recombination Specificity and Efficiency. The specificity of recombination was also verified by using the reporter *Z/AP*, which expresses alkaline phosphatase on Cre-mediated recombination (18). Cryosections (6 μm), from 1- and 6-week-old mice double heterozygous for the alleles *MLC2^{vcre}* and *Z/AP* were fixed and stained as described (18). We observed alkaline phosphatase staining in ventricular cardiomyocytes and in nodal tissue of the atria. Cardiac endothelia were not stained. Preparations enriched in cardiomyocytes were prepared from adult hearts as described (19).

Echocardiography and Aortic Banding. A two-dimensional short-axis view of the left ventricle was obtained with a 12-MHz transducer (Acuson Sequoia, Erlangen, Germany) in anesthetized mice. M-mode tracings were recorded and used to determine the diameter of the left ventricle at the end of the diastole (LVEDD) and systole (LVESD). Fractional shortening, a measure of the pumping function of the heart, corresponds to the value of (LVEDD-LVESD)/LVEDD. Statistical significance was assessed by using the Mann-Whitney test for nonparametric distributions. Abdominal aortic stenosis (banding) was performed as described (20).

Gene Expression Profiling Using Affymetrix Microarrays. P12 mouse ventricular tissue was homogenized in Trizol reagent (GIBCO); isolated total RNA was purified on RNeasy microcolumns (Qiagen, Chatsworth, CA). Biotinylated cRNA was prepared from 20 μg of total RNA, hybridized to Affymetrix GENECHIP Murine 11-K arrays, stained with streptavidin-phycoerythrin (Molecular Probes) and scanned on a laser confocal scanner (Hewlett-Packard) according to the manufacturers' instructions. Fluorescence intensity values were analyzed by using MICROARRAY SUITE 5.0 (Affymetrix) and were scaled by using a target intensity value of 1,000. Changes in gene expression between conditional mutants and controls were calculated by dividing the mean signal intensities. Statistical significance was assessed by using Student's *t* test.

Results

Distribution of the ErbB2 Receptor in the Adult Murine Heart. ErbB2 and ErbB4 mRNA and protein are produced in the adult and embryonic heart (11, 21). We found that ErbB2 and ErbB4 receptors are distributed nonhomogeneously in adult cardiomyocyte membranes. Immunoreactivity of ErbB2 and ErbB4 is associated with periodic banded structures, the T-tubular network (Fig. 1), which also stain with anti-vinculin antibodies (Fig. 1) (22). T-tubules are formed by invaginations of the sarcolemma

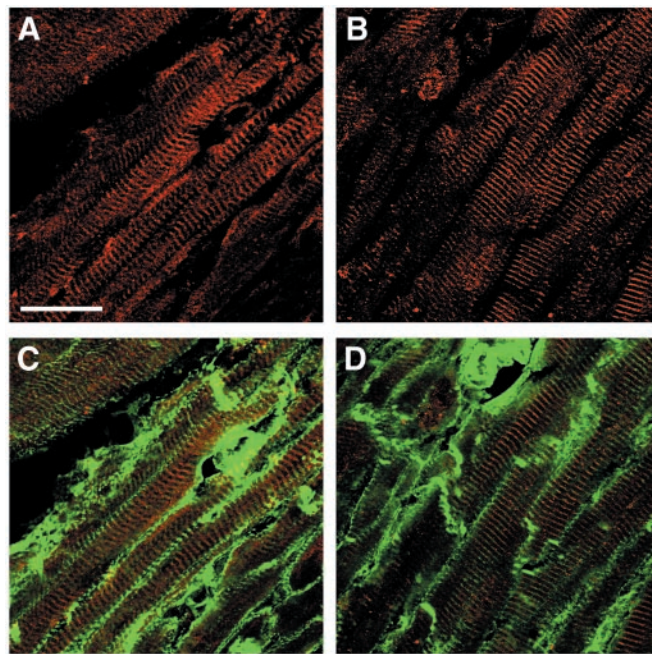


Fig. 1. ErbB2 and ErbB4 are enriched in the T-tubules of adult mouse ventricular cardiomyocytes. Cryosections were stained with antibodies against ErbB2 (A) or ErbB4 (B) and colabeled with anti-vinculin antibodies (C and D). ErbB2 (A and C, red) and ErbB4 (B and D, red) are localized in a transverse membranous network, which is also labeled by vinculin (C and D, green). T-tubular staining in longitudinal sections appears principally as transverse striations. (Bar = 25 μm .)

membrane, which remain connected to the extracellular space and in which essential components of the excitation-contraction coupling machinery are located. With shortened fixation times, ErbB2/ErbB4 staining is also observed in intercalated discs (not shown). A similar distribution of ErbB2/4 in the T-tubular system is observed also in skeletal muscle (not shown).

Cre-Induced Mutation of *ErbB2* in Cardiomyocytes. To introduce cardiomyocyte-specific mutations into *ErbB2*, we used the *MLC2^{vcre}* allele. *ErbB2^{fllox}/ErbB2^{fllox}* mice were crossed with mice heterozygous for a null mutation of *ErbB2* that also carry the *MLC2^{vcre}* allele (*MLC2^{vcre/+}; ErbB2^{+/-}*), to obtain conditional mutant mice (*MLC2^{vcre/+}; ErbB2^{fllox/-}*) (Fig. 2A; see also *Materials and Methods*). Recombination efficiencies were determined by Southern blot analysis of genomic DNA isolated from cardiomyocyte preparations of the heart ventricles. *MLC2^{vcre}* specifically introduced recombination of the *ErbB2^{fllox}* allele in 50–60% of the cardiomyocytes, resulting in a mosaicism of the heart muscle (Fig. 2B). Recombination in other tissues was not detected. Similar amounts of the recombined *ErbB2* allele were present in cardiomyocyte preparations from 5- to 6-mo-old conditional mutant (*MLC2^{vcre/+}; ErbB2^{fllox/-}*) and control (*MLC2^{vcre/+}; ErbB2^{+/-}*) mice, demonstrating that homozygous mutant cells were not preferentially lost. ErbB2 and ErbB4 protein were detectable in ventricular tissue of adult conditional mutants and controls, which contains cardiomyocytes and other cell types (Fig. 2B).

Conditional *ErbB2* Mutants Develop Severe Heart Dysfunction After Birth. In offspring from matings between *ErbB2^{fllox/fllox}* mice and *MLC2^{vcre/+}; ErbB2[±]* mice, a normal Mendelian ratio of conditional mutants was found, and thus embryonic lethality was not observed. Ventricular trabeculae of conditional *ErbB2* mutants were well developed at embryonic day (E)10.5 and E15.5, and no

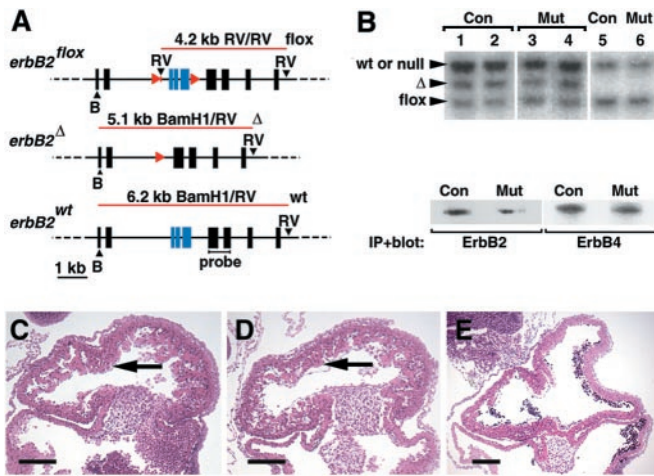


Fig. 2. Cre-mediated mutation of *ErbB2* in ventricular cardiomyocytes. (A) Schematic representation of the *ErbB2* locus, indicating restriction enzyme sites (black arrowheads: *B*, *Bam*H1; *RV*, *Eco*RV), *loxP* sequences (red arrowheads), sizes and positions of fragments obtained by digestion of genomic DNA with *Eco*RV and *Bam*H1 (red lines), and the position of the probe used for hybridization in (B). Note that the *ErbB2*^Δ allele is indistinguishable from *ErbB2*^{wt} under these conditions. (B Upper) Southern blot analysis of genomic DNA from cardiomyocyte preparations (lanes 1–4) or tails of mice (lanes 5, 6), which was digested with *Eco*RV and *Bam*H1. The genotypes were *MLC2v*^{cre/+}; *ErbB2*^{fllox/+} (control mice, lanes 1, 2, 5) or *MLC2v*^{cre/+}; *ErbB2*^{fllox/-} (conditional *ErbB2* mutant mice, lanes 3, 4, 6). Conditional mutants had markedly impaired cardiac pumping function at the time of analysis. Similar proportions of cardiomyocytes containing the recombined *ErbB2*^Δ allele were found in the ventricles of control and conditional mutant mice (lanes 1 and 2, 3 and 4, respectively), demonstrating no overt loss of *ErbB2*^Δ cardiomyocytes. (B Lower) Western blot on immunoprecipitates of ErbB2 and ErbB4 analyzed with antibodies directed against ErbB2 or ErbB4. It should be noted that entire ventricular tissue, containing cardiomyocytes and other cell types, was used for this experiment. In conditional mutants, ErbB2 protein is made by cardiomyocytes with the genotype *ErbB2*^{fllox/-}, i.e., those that escaped cre-mediated recombination, and by endothelia or other cell types that do not express *MLC2v*^{cre}. (C–E) Sections of hearts of embryonic day 10.5 embryos, stained with hematoxylin/eosin. (C) Conditional *ErbB2* mutant, and (D) control, showing normal heart histology (arrows). (E) Homozygous mutant *ErbB2*^{Δ/Δ} show the myocardial phenotype seen also in *ErbB2*^{-/-} mice, i.e., an absence of ventricular trabeculation. (Bars in C–E = 200 μm.)

morphological or histological abnormalities were observed at these stages (eight conditional mutant animals analyzed; Fig. 2 C–E and data not shown). Heart diameter and function in individual mice that reached adulthood were followed by ultrasound echocardiography over time (Fig. 3). At 1 mo of age, the average left ventricular end-diastolic diameter was similar in control and conditional mutant mice, but dilatation and a loss of contractility became marked subsequently. At the age of 3 mo, the ventricular diameter reached an average value of 4.3 mm in conditional mutants compared with 3.3 mm in control mice (Fig. 3C and data not shown). Fractional shortening, a measure of heart-pumping function, became markedly impaired in the aging conditional mutants (Fig. 3D). Moreover, ECG examination demonstrated a significantly lengthened QT_c interval (+23%, $n = 23$ vs. 15, $P = 0.014$) caused by a slowed ventricular repolarization in the conditional mutants. Thus, a progressive malfunction of the heart was observed in aging conditional *ErbB2* mutant mice. Moreover, a proportion of the conditional mutant mice died prematurely. Sudden death of conditional mutants was also observed during echocardiographic and ECG examinations, which were performed under anesthesia.

To analyze the response of conditional mutant hearts to increased stress, abdominal aortic banding was performed. This reduces the diameter of the aorta and results in stress on the

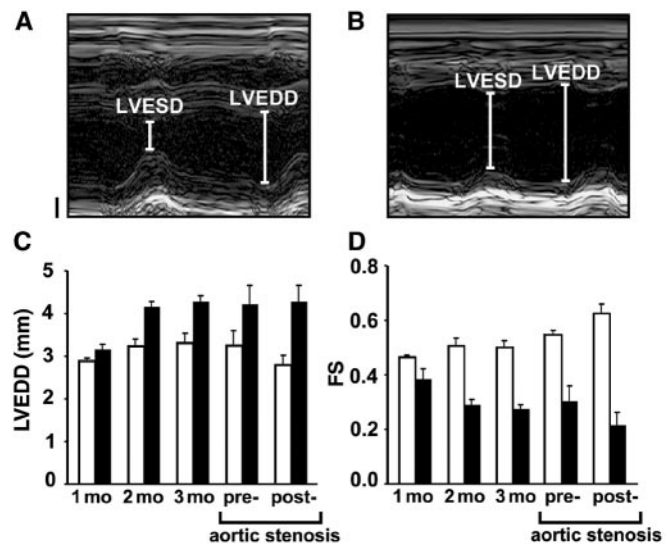


Fig. 3. Conditional *ErbB2* mutants develop marked deficits in heart function. Representative examples of ultrasound images of the left ventricle from control (A) and conditional *ErbB2* mutant (B) 3-mo-old mice used to determine left ventricular end-diastolic (LVEDD) and end-systolic diameters (LVESD). Vertical axes in A and B represent the size (Bar = 1 mm), and the horizontal axes represent a time course. (C) LVEDD and (D) fractional shortening (FS) of control animals (clear bars) and conditional *ErbB2* mutants (solid bars) of the indicated ages. Conditional mutant mice develop ventricular dilatation [1 mo, not significant (n.s.); 2 mo, $P = 0.0025$; 3 mo, $P = 0.003$] and impaired pumping function, which is reflected in reduced FS (1 mo, n.s.; 2 mo, $P = 0.0009$; 3 mo, $P = 0.0003$). Analysis of 3-mo-old conditional mutant and control mice before and 1 week after banding of the abdominal aorta (C and D) revealed a significant difference ($P = 0.03$) in the change in FS. Mean \pm SEM are depicted.

heart, which has to pump against an increased resistance. In control mice, the increased working load was compensated for by increased fractional shortening 1 wk after aortic banding (Fig. 3 C and D). In contrast, the conditional mutant hearts did not compensate after aortic banding, but displayed a further decrease in fractional shortening (Fig. 3D).

Histology of adult conditional mutant hearts revealed enlarged ventricular chambers with thinned walls, and myofiber hypertrophy (Fig. 4 A–D). In 3-mo-old conditional mutant hearts, cardiomyocytes, despite being hypertrophic, had normal myofibrillar architecture and intercellular junctions when examined by electron microscopy (Fig. 4 E and F and data not shown). However, enlarged cardiomyocyte nuclei with abnormal morphology were frequently observed. Heart-to-body-weight ratios of adult conditional mutants were increased relative to control by 26% ($n = 8$ per group, $P = 0.001$), a further indication of hypertrophy. Terminal deoxynucleotidyltransferase-mediated dUTP end labeling (TUNEL) staining did not reveal significant changes in apoptosis rates (1.4 ± 0.2 TUNEL-positive nuclei per field in adult conditional mutant and 1.1 ± 0.2 in control hearts). Apoptosis rates were also similar in adult control and conditional mutant mice 1 wk after aortic banding (1.7 ± 0.3 positive nuclei in conditional mutant and 2.2 ± 0.4 in control hearts). Cell proliferation in control and conditional mutant hearts was similar at P7, as assessed by BrdUrd incorporation (57.7 ± 2.4 BrdUrd-positive nuclei per field in conditional mutant and 61.0 ± 1.4 in control hearts).

Effect of the *ErbB2* Mutation on Gene Expression in the Hearts of Conditional Mutant Mice. To identify target genes of ErbB2 signaling in the heart, RNA was isolated from the heart ventricles of control and conditional mutant mice and analyzed by Affymetrix microarray hybridization (Table 1). To minimize effects

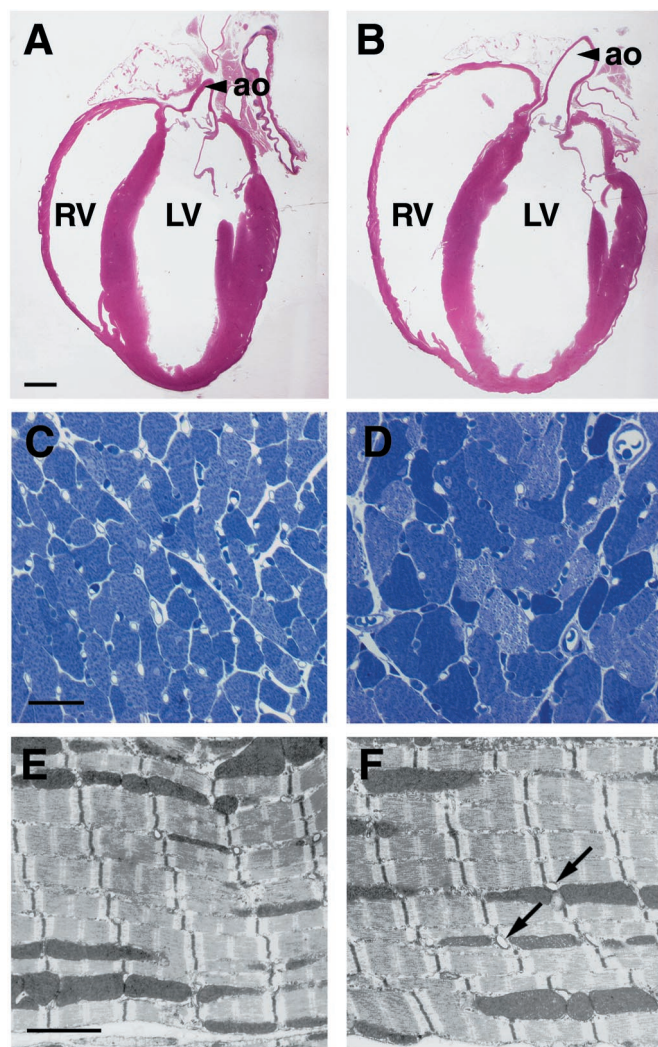


Fig. 4. Ventricular dilatation and myofiber hypertrophy in conditional *ErbB2* mutant mice. Histological (A–D) and electron microscopical analysis (E and F) of control (A, C, and E) and conditional *ErbB2* mutant mice (B, D, and F). (A and B) Hematoxylin/eosin-stained sections of the entire heart of 3-mo-old animals. Note the dilatation of both ventricular chambers (ao, aorta; RV, LV, right and left ventricle, respectively) in conditional mutants. (C and D) High magnifications of toluidine blue-stained semithin sections, with myofiber hypertrophy apparent in conditional mutants. (E and F) A normal myofibrillar ultrastructure was observed by electron microscopy in conditional mutants. Note the increased diameter of some T-tubules in the conditional mutant hearts (arrows). (Bars = A and B, 1 mm; C and D, 25 μ m; E and F, 2 μ m.)

on gene expression caused by secondary changes, conditional mutant animals were analyzed at a stage when they display no overt signs of heart dysfunction: they were 12 days old and had normal weight and heart morphology. Principally, the differences observed in gene expression between control and conditional mutant hearts were small. Genes whose expression was increased included those encoding natriuretic peptides (atrial natriuretic factor; brain natriuretic peptide) and skeletal α -actin, which are typically up-regulated in compensatory cardiac hypertrophy (Table 1; see ref. 23). We identified few additional genes whose expression was changed, such as *ATF3*. *ATF3* expression was previously reported to be up-regulated in an ischemic heart model (24), and its overexpression causes cardiac dysfunction and hypertrophy (25). Thus, the compensatory hypertrophy program commences in the hearts of conditional *ErbB2* mutant mice before obvious changes in morphology and pumping func-

tion. Little overlap exists between genes whose expression is altered in conditional *ErbB2* mutant hearts and those changed after addition of Neuregulins-1 and -2 to cultured epithelial cells (26) (see Supporting Information, which is published on the PNAS web site, www.pnas.org).

Discussion

Using conditional mutagenesis in mice, we show here that ErbB2 is essential for the normal functioning of the postnatal heart. We used Cre-*loxP*-mediated recombination to introduce the *ErbB2* mutation in ventricular cardiomyocytes and found that the conditional mutant mice acquire a severe dilated cardiomyopathy, which is associated with the occurrence of sudden death. Sudden death accompanies dilated cardiomyopathies in mice and humans and reflects secondary changes caused by tissue injuries and fibrosis, which impair the cardiac conduction system and cause arrhythmias (27). Our findings shed new light on the clinical observations of increased risk of cardiac problems in breast cancer patients that undergo an anti-ErbB2 antibody-based tumor therapy. Cardiomyopathy is also observed after conditional mutation of *ErbB4* in cardiomyocytes (Cecilia Herzig, personal communication), indicating that ErbB2 functions as an ErbB4 coreceptor in the adult heart. In general, ErbB2/ErbB4 heteromers are higher-affinity receptors than ErbB4 homomers (28). Thus, the mutation of *ErbB2* in cardiomyocytes is expected to result in decreased ErbB4 ligand binding and activation.

The reasons for the adverse effects of anti-ErbB2 antibody treatment, which can lead to heart disease, were ill understood (29). We demonstrate here that the presence of ErbB2 in cardiomyocytes is essential for adult heart function. A low incidence of cardiac dysfunction (1%) is observed in patients undergoing Trastuzumab monotherapy (30). Prior exposure to anthracyclines, which are known cardiotoxic agents, increases the incidence of cardiac side effects of a Trastuzumab monotherapy to 7%. This is alarmingly augmented to 27–29% when Trastuzumab therapy is used in combination with anthracyclines or other cytostatic agents (13, 30). Thus, Trastuzumab augments previous heart damage, and it may sensitize the cardiac system to cardiotoxic agents. Beyond the essential role in the normal heart revealed by our experiments, the ErbB2 receptor might thus function also in cardioprotective responses. Further, ErbB2 down-regulation might be facilitated in damaged hearts (see also below).

Trastuzumab binds ErbB2 and induces dimerization and down-regulation of the receptor (12). Dimerization of ErbB2 in the membrane is a first step necessary for down-regulation, and low receptor concentrations are expected to reduce the efficiency of Trastuzumab's action. Thus, antibody-mediated down-regulation of ErbB2 in tissues that express low receptor levels was expected to be marginal. ErbB receptors are clustered in discrete membrane compartments through interaction with PDZ-domain-containing proteins, such as Erbin, PSD-95, or PICK1 (31–33). We find that the ErbB2 and ErbB4 receptors in the heart are also localized to a specific membrane compartment, the T-tubule system. Despite the overall low abundance of ErbB2 in the heart, its increased local concentration might facilitate Trastuzumab's action. T-tubules, invaginations of the surface membrane with an average diameter of 250 nm, form a reticulum in striated muscle cells, which is open to the extracellular space and can be accessed by macromolecules (34). Dilatation of T-tubules, a recognized secondary change in cardiomyopathies, might facilitate access of antibodies to T-tubules in a diseased heart (35, 36). Interestingly, such T-tubular changes were also observed after anthracycline treatment (37). However, the incidence of cardiac side effects observed in patients undergoing Trastuzumab therapy is low, and the effects are thus subtle compared with the severe cardiomyopathy observed in the

Table 1. Changes in gene expression in the heart ventricle of conditional ErbB2 mutant mice

GenBank	Affymetrix accession	Description	Fold change	Control \pm SD	Mutant \pm SD	P
Hypertrophy						
*M12347	m12347_s_at	Skeletal α -actin	2.9	6538 \pm 1304	18853 \pm 2561	0.0006
*W77688	Msa.432.0_s_at	ANF	2.7	3527 \pm 637	9453 \pm 1419	0.0014
*D16497	D16497_s_at	BNP	2.2	5839 \pm 630	12919 \pm 1305	0.0004
Transcription						
D42124	d42124_s_at	MafK/NF_E2 p18	2.7	205 \pm 171	561 \pm 194	0.0338
[†] U19118	u19118_s_at	Atf3/LRG-21	2.2	259 \pm 8	562 \pm 113	0.0124
W83068	Msa.16958.0_f_at	E2F-1	-2.1	660 \pm 151	317 \pm 150	0.0180
Z16406	Z16406_s_at	Meox-2/Mox-2	-2.3	690 \pm 103	306 \pm 164	0.0104
Signaling						
AA408555	aa408555_at	Rap-2B	-2.1	549 \pm 98	265 \pm 124	0.0126
Unknown						
C81515	C81515_rc_at	EST/unknown	2.3	218 \pm 125	508 \pm 175	0.0398
AA711151	aa711151_s_at	EST/unknown	-2.6	688 \pm 232	268 \pm 133	0.0271

Gene expression in heart ventricular tissue determined by Affymetrix microarray hybridization, comparing control and conditional *ErbB2* mutants at postnatal day 12 ($n = 4$ per experimental group). Displayed are those genes for which mRNA expression changes of ≥ 2.0 ($P \geq 0.05$) occurred, and that displayed hybridization intensities of at least 500 units in control or conditional mutant tissue. GenBank and Affymetrix accession numbers and sequence descriptions are indicated. Also indicated are the fold changes in expression levels of conditional mutants relative to controls (F.Ch.), the mean hybridization signal intensities (\pm SD), and the P values. *, genes previously identified in models of cardiac hypertrophy (*ANF*, *BNP*, *actin*) (23, 48) or [†], stress (ATF3) (24). Expression of *ANF*, *BNP*, and *skeletal α -actin* was confirmed by Taqman real-time PCR, and increases of 2.98 ($P = 0.036$), 2.25 ($P = 0.002$), and 3.35 ($P = 0.010$) were determined, respectively.

conditional *ErbB2* mutant mice. Thus, in hearts of patients, only a fraction of the ErbB2 receptor pool appears to be targeted and down-regulated by the antibody.

Functions of ErbB2 in Postnatal Cardiomyocytes. Conditional *ErbB2* mutant mice display a complex cardiac phenotype, which includes hypertrophy, ventricular dilatation, and decreased pumping function. Hypertrophy in healthy individuals is the consequence of prolonged biomechanical challenge of the heart (for example, exercise) and accompanies an increased cardiac pumping function (38). Hypertrophy is also frequently observed in cardiomyopathy patients but is then combined with decreased pumping function that can lead to cardiac failure, similar to what is seen in the conditional *ErbB2* mutants. Generally, hypertrophy is an indicator for cardiac stress, whether induced by exercise or by pathological alterations. The hypertrophy observed in the conditional *ErbB2* mutant mice can thus be interpreted as a consequence of stress caused by an underlying functional deficit in the heart.

The conditional *ErbB2* mutant mice also display a lengthened time to repolarize the ventricle (increased QT_c) and an absence of tachycardia, which are not usually associated with dilated cardiomyopathy in humans. Changes in K⁺- or Na⁺-channel activity in humans and mice cause increased QT_c and *torsades de pointes* arrhythmias (39). The various symptoms in the conditional mutant mice indicate that ErbB2 takes over complex roles in the adult heart—for instance, the modulation of contractile function. ErbB receptors classically activate various signaling cascades and affect the activity of K⁺ channels, nonselective cation channels (TRPs), and G-protein-coupled receptors, all of which can impinge on heart function (40–42). Epidermal growth factor was reported to cause acute effects on ventricular contractility and heart rate in perfused rat hearts and on K⁺ currents in isolated sinus node myocytes (43, 44). ErbB receptors could interact directly with proteins of the excitation–contraction coupling machinery that also locate to T-tubules. However, an acute effect of Neuregulin-1 on the frequency of spontaneous Ca²⁺ transients in cultured neonatal or embryonic cardiomyocytes was not seen (A.N.G., unpublished observations). It is interesting to note that in cultured human and rat cardiomyo-

cytes, prolonged treatment with anti-ErbB2 antibody causes atrophy and a loss of contractile function, which can be overcome by long-term exposure to Neuregulins (Jay Schneider and Cary Lai, personal communication).

Loss of cardiomyocytes can also induce cardiac stress and can result in impaired pumping and hypertrophy (19, 45). Neuregulin/ErbB signaling increases survival of cultured postnatal cardiomyocytes (46), and Neuregulin-1 in combination with insulin-like growth factor I can enhance cardiomyocyte proliferation during development (47). In the hearts of the adult conditional *ErbB2* mutants, we did not detect significantly increased apoptosis or changes in proliferation of cardiomyocytes. Aortic banding has revealed in other models effects on the survival of cardiomyocytes (19) but did not change apoptosis rates in conditional *ErbB2* mutant mice. Furthermore, a preferential loss of homozygous *ErbB2* mutant cardiomyocytes was not observed. It was possible to assess such a loss because recombination induced by Cre was not complete, resulting in a mosaicism of homozygous and heterozygous mutant cardiomyocytes in conditional mutants. The two cell types are present in similar proportions in newborn and adult hearts. Thus, mechanisms distinct from apoptosis appear to cause cardiomyopathy in conditional *ErbB2* mutants, such as impaired contractility.

Gene Expression in the Heart of Conditional *ErbB2* Mutant Mice. We found that expression of natriuretic peptides [atrial natriuretic factor (ANF), brain natriuretic peptide (BNP)] and skeletal α -actin is increased in the hearts of the conditional *ErbB2* mutants. Up-regulation in the expression of ANF, BNP, and actin has been previously noted in various models of cardiac hypertrophy or cardiac dysfunction (23, 48). These genes are also expressed at high levels in the developing heart, and their up-regulation in pathology was suggested to reflect a return to the embryonic gene expression program (23). The expression of genes encoding cyclin G, desmoplakin 1, insulin-like growth factor II, protein phosphatase 1 γ (PP1 γ), and pro-collagen 1 were reported as changed in hypertrophy previously (23, 48) but were not altered in our model (see Supporting Information on the PNAS web site). Some of the observed differences might reflect the distinct etiologies of the hypertrophy in the respective

models. Eventually, expression profiling may allow the correlation of genetic and/or environmental causes of cardiomyopathies with alterations in gene expression. The activation of the hypertrophy program in conditional *ErbB2* mutants most likely reflects a secondary response that is induced by cardiac stress resulting from impaired ErbB2 signaling.

We thank S. Schmidt, A. Leschke, T. Schalow, K. Gottschling, S. Buchert, and C. Rudolph for expert technical assistance. We are indebted to H.

Schulz and J. Monti (MDC, Berlin) for assistance with the analysis of Affymetrix GENECHIP data and Taqman real-time PCR data. We also thank C. Lindschau (FVK, Berlin) for advice and supervision on Fura-2 imaging of cardiomyocytes, G. Wallukat and M. Wegener (MDC, Berlin) for providing cultures of rat cardiomyocytes, as well as R. Dietz (FVK, Berlin) and W. Birchmeier (MDC, Berlin) for critical reading of the manuscript. This work was funded by a grant from the Volkswagen Foundation (to C.B.) and a clinical cooperation grant from the M.D.C. (to C.B. and C.Ö.).

- Seidman, J. G. & Seidman, C. (2001) *Cell* **104**, 557–567.
- Towbin, J. A. (1998) *Curr. Opin. Cell Biol.* **10**, 131–139.
- Emanuelli, C., Maestri, R., Corradi, D., Marchione, R., Minasi, A., Tozzi, M. G., Salis, M. B., Straino, S., Capogrossi, M. C., Olivetti, G. & Madeddu, P. (1999) *Circulation* **100**, 2359–2365.
- Nebigil, C. G., Hickel, P., Messaddeq, N., Vonesch, J. L., Douchet, M. P., Monassier, L., Gyorgy, K., Matz, R., Andriantsitohaina, R., Manivet, P., et al. (2001) *Circulation* **103**, 2973–2979.
- Kiriazis, H. & Kranias, E. G. (2000) *Annu. Rev. Physiol.* **62**, 321–351.
- Yarden, Y. & Sliwkowski, M. X. (2001) *Nat. Rev. Mol. Cell Biol.* **2**, 127–137.
- Bange, J., Zwick, E. & Ullrich, A. (2001) *Nat. Med.* **7**, 548–552.
- Lemke, G. (1996) *Mol. Cell. Neurosci.* **7**, 247–262.
- Garratt, A. N., Britsch, S. & Birchmeier, C. (2000) *BioEssays* **22**, 987–996.
- Gschwind, A., Zwick, E., Prenzel, N., Leserer, M. & Ullrich, A. (2001) *Oncogene* **20**, 1594–1600.
- Meyer, D. & Birchmeier, C. (1995) *Nature (London)* **378**, 386–390.
- Sliwkowski, M. X., Lofgren, J. A., Lewis, G. D., Hotaling, T. E., Fendly, B. M. & Fox, J. A. (1999) *Semin. Oncol.* **26**, 60–70.
- Slamon, D. J., Leyland-Jones, B., Shak, S., Fuchs, H., Paton, V., Bajamonde, A., Fleming, T., Eiermann, W., Wolter, J., Pegram, M., et al. (2001) *N. Engl. J. Med.* **344**, 783–792.
- Chen, J., Kubalak, S. W., Minamisawa, S., Price, R. L., Becker, K. D., Hickey, R., Ross, J., Jr. & Chien, K. R. (1998) *J. Biol. Chem.* **273**, 1252–1256.
- Minamisawa, S., Gu, Y., Ross, J., Jr., Chien, K. R. & Chen, J. (1999) *J. Biol. Chem.* **274**, 10066–10070.
- Garratt, A. N., Voiculescu, O., Topilko, P., Charnay, P. & Birchmeier, C. (2000) *J. Cell. Biol.* **148**, 1035–1046.
- Britsch, S., Li, L., Kirchhoff, S., Theuring, F., Brinkmann, V., Birchmeier, C. & Riethmacher, D. (1998) *Genes Dev.* **12**, 1825–1836.
- Lobe, C. G., Koop, K. E., Kreppner, W., Lomeli, H., Gertsenstein, M. & Nagy, A. (1999) *Dev. Biol.* **208**, 281–292.
- Hirota, H., Chen, J., Betz, U. A., Rajewsky, K., Gu, Y., Ross, J., Jr., Muller, W. & Chien, K. R. (1999) *Cell* **97**, 189–198.
- Wettschreck, N., Rutten, H., Zywietz, A., Gehring, D., Wilkie, T. M., Chen, J., Chien, K. R. & Offermanns, S. (2001) *Nat. Med.* **7**, 1236–1240.
- Rohrbach, S., Yan, X., Weinberg, E. O., Hasan, F., Bartunek, J., Marchionni, M. A. & Lorell, B. H. (1999) *Circulation* **100**, 407–412.
- Kostin, S., Scholz, D., Shimada, T., Maeno, Y., Mollnau, H., Hein, S. & Schaper, J. (1998) *Cell Tissue Res.* **294**, 449–460.
- Friddle, C. J., Koga, T., Rubin, E. M. & Bristow, J. (2000) *Proc. Natl. Acad. Sci. USA* **97**, 6745–6750.
- Chen, B. P., Wolfgang, C. D. & Hai, T. (1996) *Mol. Cell Biol.* **16**, 1157–1168.
- Okamoto, Y., Chaves, A., Chen, J., Kelley, R., Jones, K., Weed, H. G., Gardner, K. L., Gangi, L., Yamaguchi, M., Klomkleaw, W., et al. (2001) *Am. J. Pathol.* **159**, 639–650.
- Sweeney, C., Fambrough, D., Huard, C., Diamonti, A. J., Lander, E. S., Cantley, L. C. & Carraway, K. L., 3rd (2001) *J. Biol. Chem.* **276**, 22685–22698.
- Brandenburg, R. O. (1985) *J. Am. Coll. Cardiol.* **5**, 185B–189B.
- Jones, J. T., Akita, R. W. & Sliwkowski, M. X. (1999) *FEBS Lett.* **447**, 227–231.
- Ewer, M. S., Gibbs, H. R., Swafford, J. & Benjamin, R. S. (1999) *Semin. Oncol.* **26**, 96–101.
- Sparano, J. A. (2001) *Semin. Oncol.* **28**, 20–27.
- Borg, J. P., Marchetto, S., Le Bivic, A., Ollendorff, V., Jaulin-Bastard, F., Saito, H., Fournier, E., Adelaide, J., Margolis, B. & Birnbaum, D. (2000) *Nat. Cell Biol.* **2**, 407–414.
- Carraway, K. L., 3rd & Sweeney, C. (2001) *Curr. Opin. Cell Biol.* **13**, 125–130.
- Jaulin-Bastard, F., Saito, H., Le Bivic, A., Ollendorff, V., Marchetto, S., Birnbaum, D. & Borg, J. P. (2001) *J. Biol. Chem.* **276**, 15256–15263.
- Soeller, C. & Cannell, M. B. (1999) *Circ. Res.* **84**, 266–275.
- Carrasco Guerra, H. A., Palacios-Pru, E., Dagert de Scorza, C., Molina, C., Inglessis, G. & Mendoza, R. V. (1987) *Am. Heart J.* **113**, 716–724.
- Schaper, J., Froede, R., Hein, S., Buck, A., Hashizume, H., Speiser, B., Friedl, A. & Bleese, N. (1991) *Circulation* **83**, 504–514.
- Unverferth, D. V., Magorien, R. D., Unverferth, B. P., Talley, R. L., Balcerzak, S. P. & Baba, N. (1981) *Cancer Treat. Rep.* **65**, 1093–1097.
- Hunter, J. J. & Chien, K. R. (1999) *N. Engl. J. Med.* **341**, 1276–1283.
- Keating, M. T. & Sanguinetti, M. C. (2001) *Cell* **104**, 569–580.
- Wischmeyer, E., Doring, F. & Karschin, A. (1998) *J. Biol. Chem.* **273**, 34063–34068.
- Prenzel, N., Zwick, E., Daub, H., Leserer, M., Abraham, R., Wallasch, C. & Ullrich, A. (1999) *Nature (London)* **402**, 884–888.
- Schaefer, M., Plant, T. D., Obukhov, A. G., Hofmann, T., Gudermann, T. & Schultz, G. (2000) *J. Biol. Chem.* **275**, 17517–17526.
- Nair, B. G., Rashed, H. M. & Patel, T. B. (1993) *Growth Factors* **8**, 41–48.
- Wu, J. Y., Yu, H. & Cohen, I. S. (2000) *Biochim. Biophys. Acta* **1463**, 15–19.
- Chien, K. R. (1999) *Cell* **98**, 555–558.
- Zhao, Y. Y., Sawyer, D. R., Baliga, R. R., Opel, D. J., Han, X., Marchionni, M. A. & Kelly, R. A. (1998) *J. Biol. Chem.* **273**, 10261–10269.
- Hertig, C. M., Kubalak, S. W., Wang, Y. & Chien, K. R. (1999) *J. Biol. Chem.* **274**, 37362–37369.
- Johnatty, S. E., Dyck, J. R., Michael, L. H., Olson, E. N. & Abdellatif, M. (2000) *J. Mol. Cell. Cardiol.* **32**, 805–815.